0026-895X/06/6903-823–832$20.00
MOLECULAR PHARMACOLOGY
Vol. 69, No. 3
18127/3083567
Mol Pharmacol 69:823–832, 2006
Printed in U.S.A.

Block of Peripheral Nerve Sodium Channels Selectively Inhibits Features of Neuropathic Pain in Rats

Richard M. Brochu, Ivy E. Dick, Jason W. Tarpley, Erin McGowan, David Gunner, James Herrington, Pengcheng P. Shao, Dong Ok, Chunshi Li, William H. Parsons, Gary L. Stump, Christopher P. Regan, Joseph J. Lynch, Jr., Kathryn A. Lyons, Owen B. McManus, Samantha Clark, Zahid Ali, Gregory J. Kaczorowski, William J. Martin, and Birgit T. Priest

Departments of Ion Channels (R.M.B., I.E.D., J.H., O.B.M., G.J.K., B.T.P.), Pharmacology (J.W.T., E.M., W.J.M.), Medicinal Chemistry (P.P.S., D.O., C.L., K.A.L., W.H.P.), and Cardiovascular Disease (G.L.S., C.P.R., J.J.L.); Merck Research Laboratories, Rahway, New Jersey; and Merck Sharp and Dohme Research Laboratories, Neuroscience Research Centre, Terlings Park, Harlow, Essex, United Kingdom (D.G., S.C., Z.A.)

Received August 16, 2005; accepted November 16, 2005

ABSTRACT

Several sodium channel blockers are used clinically to treat neuropathic pain. However, many patients fail to achieve adequate pain relief from these highly brain-penetrant drugs because of dose-limiting central nervous system side effects. Here, we describe the functional properties of *trans*-*N*-{[2′-(aminosulfonyl)biphenyl-4-yl]methyl}-*N*-methyl-*N*′-[4-(trifluoromethoxy)benzyl]cyclopentane-1,2-dicarboxamide (CDA54), a peripherally acting sodium channel blocker. In whole-cell electrophysiological assays, CDA54 blocked the inactivated states of $hNa_V1.7$ and $hNa_V1.8$, two channels of the peripheral nervous system implicated in nociceptive transmission, with affinities of 0.25 and 0.18 μM, respectively. CDA54 displayed similar affinities for the tetrodotoxin-resistant Na^+ current in small-diameter mouse dorsal root ganglion neurons. Peripheral nerve injury causes spontaneous electrical activity in normally silent sensory neurons. CDA54 inhibited these injury-induced spontaneous action potentials at concentrations 10-fold lower than those required to block normal A- and C-fiber conduction. Consistent with the selective inhibition of injury-induced firing, CDA54 (10 mg/kg p.o.) significantly reduced behavioral signs of neuropathic pain in two nerve injury models, whereas the same dose of CDA54 did not affect acute nociception or motor coordination. In anesthetized dogs, CDA54, at plasma concentrations of 6.7 μM, had no effect on cardiac electrophysiological parameters including conduction. Thus, the peripheral nerve sodium channel blocker CDA54 selectively inhibits sensory nerve signaling associated with neuropathic pain.

The anticonvulsants carbamazepine and lamotrigine and the antiarrhythmics lidocaine and mexiletine are used clinically to treat neuropathic pain. They are state-dependent sodium channel blockers, binding primarily to the open and inactivated states of the channel (Hille, 1977; Hondeghem and Katzung, 1977). As channels accumulate in the drug-bound inactivated state, fewer channels are available to open upon membrane depolarization, leading to slowing and eventually to the block of action potential conduction. Because of the voltage dependence of inactivation, this form of state-dependent block results in preferential inhibition of action potentials in rapidly firing or partially depolarized cells, contributing to the therapeutic index of anticonvulsants and antiarrhythmics (Clare et al., 2000).

In animal models of neuropathic pain, damage to primary afferent sensory neurons can lead to spontaneous action potential firing in normally silent sensory neurons, and these ectopic discharges are believed to contribute to the generation and maintenance of neuropathic pain (Kajander and Bennett, 1992). In rat models of peripheral nerve injury, the onset of ectopic action potential firing in the injured nerve corresponds to the onset of behavioral signs of pain, such as mechanical allodynia (Liu et al., 2000). In these models,

R.M.B. and I.E.D. contributed equally to this work.

Article, publication date, and citation information can be found at http://molpharm.aspetjournals.org.
doi:10.1124/mol.105.018127.

ABBREVIATIONS: CDA54, *trans*-*N*-{[2′-(aminosulfonyl)biphenyl-4-yl]methyl}-*N*-methyl-*N*′-[4-(trifluoromethoxy)benzyl]cyclopentane-1,2-dicarboxamide; DRG, dorsal root ganglion; BAPTA, 1,2-bis(2-aminophenoxy)ethane-*N,N,N*′,*N*′-tetraacetic acid; CCI, chronic constriction injury; Na_V, voltage-dependent sodium channel; SIF, synthetic interstitial fluid; SNL, spinal nerve ligation; ANOVA, analysis of variance; HEK, human embryonic kidney; SIF, synthetic interstitial fluid; h, human.

intravenous application of lidocaine, at clinically relevant doses, suppresses the ectopic discharges and reverses mechanical allodynia without affecting general behavior and motor function (Chaplan et al., 1995). These results suggest that a sodium channel blocker with the appropriate properties may be able to selectively inhibit sensory nerve action potentials associated with an injury-induced sensitized state. Indeed, systemically administered lidocaine has been shown to be effective in the treatment of several neuropathic pain disorders at doses that do not produce anesthesia or slow cardiac conduction (Tanelian and Brose, 1991). More recently, lidocaine has been formulated as a dermal patch (Lidoderm, Endo Pharmaceuticals, Chadds Ford, PA), and this formulation has been approved by the Food and Drug Administration for the treatment of postherpetic neuralgia (Devers and Galer, 2000). Although lidocaine is highly brain-penetrant (Nakazono et al., 1991), the low systemic concentrations achieved by transdermal lidocaine application suggest that efficacy is achieved via block of peripheral rather than central nervous system sodium channels.

Several Na_V1 subtypes are expressed in the peripheral nervous system, and the preferential expression of $Na_V1.7$, $Na_V1.8$, and $Na_V1.9$ in nociceptive neurons suggests a role of these subtypes in pain transmission. Mutations in $Na_V1.7$ have been linked to primary erythermalgia, a human heritable disease associated with episodes of burning pain (Yang et al., 2004), and phenotyping of mice carrying a nociceptor-specific deletion of the $Na_V1.7$ gene has provided evidence for a role of this sodium channel subtype in mediating inflammatory pain signaling (Nassar et al., 2004). $Na_V1.8$ is responsible for the majority of the inward current during action potentials in small-diameter neurons (Renganathan et al., 2001), and evidence from experiments in rats using antisense oligonucleotides indicates a role of this channel in neuropathic (Lai et al., 2002), inflammatory (Khasar et al., 1998), and visceral (Yoshimura et al., 2001) pain. Despite a compensatory up-regulation of tetrodotoxin-sensitive sodium current, $Na_V1.8$ null mutant mice displayed reduced sensitivity to inflammatory hyperalgesia (Akopian et al., 1999; Laird et al., 2002). Finally, $Na_V1.9$ null mutant mice provide evidence that the $Na_V1.9$ subtype also contributes to inflammatory pain signaling (Priest et al., 2005).

Here, we examine the in vitro mechanism of action, the effect on sensory nerve firing, and the analgesic properties of *trans*-*N*-{[2′-(aminosulfonyl)biphenyl-4-yl]methyl}-*N*-methyl-*N*′-[4-(trifluoromethoxy)benzyl]cyclopentane-1,2-dicarboxamide (CDA54) (Shao et al., 2005), an orally active sodium channel blocker with an assumed peripheral site of action.

Materials and Methods

Animals. All procedures involving animals were carried out in accordance with the United Kingdom Animals (Scientific Procedures) Act of 1986 or the National Institutes of Health guidelines for the use of live animals and were approved by the Merck Research Laboratories Institutional Animal Care and Use Committee. Rats were maintained in a temperature-controlled (23°C) facility with a 12-h light/dark cycle and had ad libitum access to water and regular rodent chow.

Plasma and Brain Concentrations. Plasma and brain concentrations of CDA54 were determined by liquid chromatography-mass spectrometry/mass spectrometry using an API 3000 mass spectrometer (Applied Biosystems/MDS Sciex, Foster City, CA) operated in positive ion atmospheric pressure chemical ionization mode with multiple-reaction monitoring. Plasma was prepared for analysis by solid-phase extraction using OASIS HLB extractions plates (30 mg; Waters Corporation, Milford, MA), and brain homogenate (1:3 tissue/water) was prepared by protein precipitation with acetonitrile. Extracts were chromatographed using a DuPont Zorbax SB-C18 column (50 × 2 mm, 5 μm; DuPont, Wilmington, DE) and eluted at 0.2 ml/min under isocratic conditions with acetonitrile/water (85:15) containing 5 mM ammonium formate/0.1% formic acid. Under these conditions, CDA54 eluted at 3.5 min.

Dorsal Root Ganglion Preparation. Dorsal root ganglia (DRGs) were dissected from BKTO mice after cervical dislocation. Ganglia from all levels were placed into Hanks' solution containing 45 units/ml papain and 0.4 mg/ml L-cysteine for 15 min at 37°C, followed by 2 mg/ml collagenase (type I) in Hanks' solution for 15 to 18 min at 37°C. The ganglia were washed once with growth media [F14, 10% horse serum, penicillin/streptomycin (5000 IU/500 μg), 120 mg $NaHCO_3$, and 100 ng/ml nerve growth factor] and triturated with a fire-polished pipette to obtain a single cell suspension that was plated onto poly-L-ornithine-coated glass coverslips. All recordings were made within 2 to 8 h of ganglia isolation.

Electrophysiology. Sodium currents were examined by whole-cell voltage clamp (Hamill et al., 1981) using either an EPC-9 amplifier and Pulse software (HEKA Electronics, Lambrecht/Pfalz, Germany) or an Axopatch 200B amplifier and pClamp7 software (Molecular Devices, Sunnyvale, CA). Electrodes were fire-polished to resistances of 1.5 to 4 MΩ. Voltage errors were minimized by series resistance compensation (75–85%), and the capacitance artifact was canceled using the amplifier's built-in circuitry. Data were acquired at 10 to 50 kHz and filtered at 5 to 10 kHz. For recombinant channels expressed in HEK cells, the bath solution typically consisted of 40 mM NaCl, 120 mM *N*-methyl-D-glucamine chloride, 1 mM KCl, 2.7 mM $CaCl_2$, 0.5 mM $MgCl_2$, and 10 mM *N*-methyl-D-glucamine HEPES, pH 7.4, and the internal (pipette) solution contained 110 mM, cesium methanesulfonate, 5 mM NaCl, 20 mM CsCl, 10 mM CsF, 10 mM BAPTA (tetra cesium salt), and 10 mM cesium-HEPES, pH 7.4. In some cases, *N*-methyl-D-glucamine chloride in the bath solution was replaced by NaCl to increase current amplitudes. To isolate tetrodotoxin-resistant Na^+ current in DRG neurons, the bath solution contained 40 mM NaCl, 50 mM tetraethylammonium chloride, 40 mM choline chloride, 0.1 mM $CaCl_2$, 3.9 mM $MgCl_2$, 10 mM tetraethylammonium-HEPES, 11 mM glucose, and 300 nM tetrodotoxin, pH 7.4, and the internal solution contained 115 mM CsF, 10 mM NaCl, 3.9 mM $MgCl_2$, 10 mM BAPTA (tetracesium salt), and 10 mM cesium-HEPES, pH 7.3, adjusted to 300 mOsm with sucrose. Liquid junction potentials were less than 4 mV and were not corrected for. Unless otherwise stated, the holding potential was −90 mV.

Data Analysis. All averaged data are presented as mean ± S.E. Statistical comparisons were made using Student's *t* test, and differences were considered significant at $p < 0.05$.

Chronic Constriction Injury. Neuropathic pain behavior was assessed using the chronic constriction injury (CCI) model as described by Bennett and Xie (1988). Male Sprague-Dawley rats (150–200 g) were anesthetized with halothane, and the sciatic nerve was exposed at mid-thigh level and loosely tied with four chromic catgut sutures spaced approximately 3 mm apart. The incision was sutured, and the rats were allowed to recover. After 2 weeks, the rats were either tested for mechanical hyperalgesia or euthanized by cervical dislocation after a rising concentration of carbon dioxide for in vitro electrophysiological recordings of the injured sciatic nerve. Mechanical hyperalgesia was assessed using a Ugo Basile apparatus (Stoelting Company, Wood Dale, IL). Paw pressure, applied to the injured (ipsilateral) or uninjured (contralateral) hindpaw, was increased linearly until the animal vocalized, withdrew the paw, or struggled. Two baseline measures were taken (1 h apart) before drug treatment. Rats rested for 3 h before drug treatment, and hyperalgesia was again evaluated 1 h after compound dose for mexiletine and 2 h

after dose for CDA54. The mean of the two pretreatment values was used in subsequent analyses. The antihyperalgesic response was calculated as the difference between mechanical thresholds of the injured (ipsilateral) and the uninjured (contralateral) paw. For statistical assessment, pre- and post-treatment thresholds were compared using parametric *t* tests.

In Vitro Teased-Fiber Recording. Sciatic nerves from injured and noninjured rats were dissected and placed in cold (4°C) synthetic interstitial fluid (SIF). Nerves were denuded of the perineurium, epineurium, and ligatures (injured nerves) and placed into a three-chambered perfusion bath. The middle chamber was used for drug delivery and was continuously perfused with SIF heated to 37°C. In the recording chamber, teased-fiber recordings were carried out using standard electrophysiological techniques (Campbell and Meyer, 1983). In brief, the sciatic nerve was teased into small filaments suitable for recording activity from single nerve fibers. The neural signal was differentially amplified, filtered, and digitized at a rate of 25 kHz. A real-time computer-based data acquisition and processing system (DAPSYS; the Johns Hopkins University, Baltimore, MD) was used to sort different action potential waveforms. A- and C-fiber compound action potentials were elicited by electrical stimulation at an intensity 20% greater than C-fiber threshold. All data were recorded on a CED 1401/Spike 2 data acquisition system (Cambridge Electronic Design, Cambridge, UK) and analyzed using preprogrammed scripts. For all experiments, CDA54 was dissolved in dimethyl sulfoxide and diluted into SIF so that the final concentration of dimethyl sulfoxide was 0.1%. To quantify the effects on A- and C-fiber conduction, the nerve was stimulated at 0.1 Hz and superfused with SIF for 15 min, followed by consecutive 15-min applications of vehicle (SIF + 0.1% dimethyl sulfoxide), followed by 3, 10, and 30 μM CDA54. The average (more than 1 min) A-fiber amplitude and area under the C-fiber compound action potential were determined for each compound application and normalized to the baseline response. To quantify the effects on injury-induced spontaneous activity, filaments with regular spontaneous activity were identified. After a baseline recording of 15 min, vehicle, 1 μM CDA54, and 3 μM CDA54 were applied sequentially for 15 min each. The total number of action potentials during each drug application was recorded and normalized to the baseline period. Statistical significance was determined using a one-way analysis of variance (ANOVA) followed by a Newman- Keuls multiple comparison test.

Spinal Nerve Ligation. Animals were anesthetized with isoflurane and were placed on a heating pad. Using aseptic technique, the L5 spinal nerve was exposed, ligated, and transected as described previously (Kim and Chung, 1992). Muscle and skin were closed with 4-0 polydiaxone and wound clips, respectively. Upon recovery, tactile allodynia was assessed with calibrated von Frey filaments (Stoelting Company) using an up-down paradigm (Chaplan et al., 1994) before and 1 week after nerve injury. Animals were placed in plastic cages with a wire-mesh floor and allowed to acclimate for 15 to 45 min before each test session. To determine the 50% response threshold, the von Frey filaments (over a range of intensities from 0.4 to 28.8 g) were applied to the mid-plantar surface for 8 s or until a withdrawal response occurred. After a positive response, an incrementally weaker stimulus was tested. If there was no response to a stimulus, an incrementally stronger stimulus was presented. After the initial threshold crossing, this procedure was repeated for four stimulus presentations per animal per test session. Mechanical sensitivity was then assessed at 45 and 90 min after oral administration of CDA54, and the maximum reversal was used to calculate the percentage of maximal possible effect using the following equation: (post-CDA54 − post-SNL)/(pre-SNL − post-SNL) × 100, where 100% is equivalent to the complete reversal of allodynia (i.e., preinjury value).

Rotorod Test. Motor coordination was assessed using an accelerating rotorod (Ugo Basile model 7700). Before drug treatment, rats were trained to walk continuously for 2 min on a 6-cm rotating cylinder (set at a constant speed of 10 rpm). For the testing phase, animals (n = 6/group) were placed onto the apparatus 60 to 75 min after oral administration of vehicle or CDA54. The rotorod was then accelerated, and total walking time was recorded.

Hot-Plate Test. Male Sprague-Dawley rats (170–260 g; Charles River Breeding Laboratories, Portage, MI) were placed on a 52.5°C hot plate, and the latency to hindpaw licking was measured. Three baseline values 10 min apart were taken before oral administration of CDA54 (n = 6), and rats were tested again 1 h after CDA54 administration. A 30-s cutoff latency was used to avoid tissue injury. Paired *t* tests (pre- versus postdose) were used to determine statistical significance.

Electrocardiogram and Cardiac Electrophysiological Effects. The surgical preparation and methods for the measurement of cardiac electrophysiological parameters in anesthetized dog have been described previously (Stump et al., 2003). Two groups of three animals each received two sequential intravenous doses of 0.25 and 2.5 mg/kg CDA54 or matching volume of vehicle (20% ethanol, 30% polyethylene glycol-400, and 50% water). Each dose of CDA54 was infused intravenously over a period of 5 min, with electrocardiogram and cardiac electrophysiology parameters measured 5 min after the end of infusion. Blood samples were obtained at the time of electrocardiogram and cardiac electrophysiology measurements. Data were expressed as mean ± S.E.M. Statistical significance was determined using a two-way ANOVA.

Materials. HEK-293 cell lines stably expressing $hNa_V1.2$ or $hNa_V1.8$ together with the sodium channel β1 subunit were established in-house. Stable HEK-293 cell lines expressing $hNa_V1.5$ or $hNa_V1.7$ (α subunit only) were obtained from Dr. Hartman and Aurora Biosciences (San Diego, CA), respectively. All tissue culture media were from Invitrogen (Carlsbad, CA). For electrophysiological recordings, cells were plated on 3 × 3-mm glass coverslips coated with poly-D-lysine. CDA54 was synthesized at Merck Research Laboratories (West Point, PA) (Shao et al., 2005). For in vivo experiments, with the exception of the cardiovascular studies, CDA54 was prepared in 0.5% methylcellulose and administered orally. Gabapentin and mexiletine (both from Sigma-Aldrich, St. Louis, MO) were administered in 10% hydroxypropyl-β-cyclodextrin in water and in saline, respectively.

Results

A high-throughput screening campaign discovered the novel sodium channel blocker *N*-{[2′-(aminosulfonyl)biphenyl-4-yl]methyl}-*N*′-(2,2′-bithien-5-ylmethyl)succinamide (Priest et al., 2004). *N*-{[2′-(Aminosulfonyl)biphenyl-4-yl]-methyl}-*N*′-(2,2′-bithien-5-ylmethyl)succinamide had efficacy in an animal model of tonic pain, but its poor pharmacokinetic profile prohibited further in vivo characterization. A medicinal chemistry effort yielded CDA54 (**c**yclopentane **d**icarbox**a**mide; Shao et al., 2005), shown in Fig. 1A. Dosed orally in rats, CDA54 was 44% bioavailable. A dose of 2 mg/kg produced maximal plasma concentrations of 0.93 ± 0.11 μM 1 h after dose and a half-life of approximately 1 h (Fig. 1B). Plasma concentrations of CDA54 were dose-proportional between 0.3 and 10 mg/kg p.o., and brain concentrations were 33-fold lower than plasma concentrations (Fig. 1C). The brain-to-plasma ratio produced by CDA54 was the same 2.5 h after a single 1 mg/kg dose (0.03 ± 0.02, n = 8) and 3.5 h after the fifth dose of 10 mg/kg twice-daily dosing (0.03 ± 0.01, n = 8). In contrast, mexiletine was highly brain-penetrant, producing brain-to-plasma ratios in rats of 25 and 14, 0.25 h and 4 h after 1 mg/kg i.v. dosing, respectively (data not shown), similar to published brain-to-plasma ratios of 23 (Igwemezie et al., 1992).

Block of Recombinant $Na_V1.7$ Channels by CDA54. Block of $Na_V1.7$ channels by CDA54 was examined by whole-

cell electrophysiology in stably transfected HEK-293 cells. Figure 2A shows the peak current evoked by 6-ms depolarizations to 0 mV from either −100 or −70 mV. At a holding potential of −70 mV, where 25% of $Na_V1.7$ channels were inactivated, as evidenced by the reduced current in comparison to the holding potential of −100 mV, bath application of 1 μM CDA54 blocked approximately 40% of the current. After returning the holding potential to −100 mV, $Na_V1.7$ channels apparently recovered from block by CDA54, as the current slowly returned to 85% of its amplitude before the addition of CDA54. After returning the holding potential to −70 mV, block redeveloped over a time course of several minutes (τ = 110 s). Traces shown below the time course represent the current in response to a 6-ms depolarizing pulse in control and after equilibration with 1 μM CDA54 from holding potentials of −70 mV on the left and −100 mV on the right. Figure 2B shows the average fractional block of $Na_V1.7$ current by CDA54 when the compound was applied at −100 or −70 mV (n = 3–8 for each data point). Fitting the data to the Hill equation with a Hill coefficient of 1 yielded IC_{50} values of 11.4 and 0.73 μM for holding potentials of −100 and −70 mV, respectively. CDA54 is not charged, and the dependence of block on holding potential is consistent with preferential block of channels in the inactivated state. According to the modulated receptor hypothesis (Hille, 1977), the overall affinity of CDA54 for $hNa_V1.7$ at a given membrane potential can be treated as a weighted average of the affinity of the compound for the resting and inactivated states of the channel: $K_{app} = 1/[h/K_r + (1 - h)/K_i]$, where h is the fraction of channels residing in the resting state, and K_r and K_i are the dissociation constants for the resting and inactivated channels, respectively (Kuo and Bean, 1994). At −100 mV, essentially all $hNa_V1.7$ channels reside in the resting state, and the IC_{50} value for CDA54 at this potential is assumed to reflect binding to resting channels (K_r = 11.4 μM). Under the experimental conditions used, the midpoint of steady-state inactivation of $hNa_V1.7$ channels was −67.8 ± 0.4 mV (n = 107), and at −70 mV, an average of 59% of channels were in the resting state. Assuming that the more potent block of $hNa_V1.7$ channels at −70 mV reflects preferential binding to inactivated channels, the affinity of CDA54 for inactivated channels (K_i) can then be calculated from the K_{app} at −70 mV. The data shown in Fig. 2B yielded an IC_{50} or K_{app} value of 0.73 μM at −70 mV, resulting in a K_i of 0.30 μM. When K_i was calculated separately for each experiment, the average value was 0.25 ± 0.02 μM (n = 17). In comparison, the K_i for mexiletine under the same conditions was 10.8 ± 1.7 μM (n = 3).

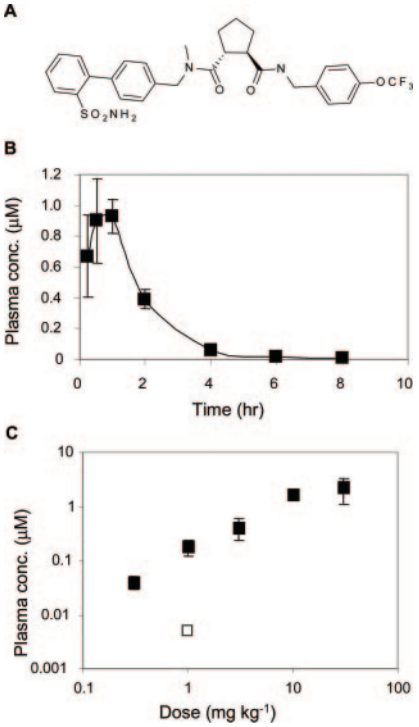

Fig. 1. A, chemical structure of CDA54. B, plasma concentration of CDA54 in rats after a single oral dose of 2 mg/kg in dimethyl sulfoxide/polyethylene glycol-400/water (15:45:40, v/v/v), expressed as mean ± S.E. (n = 3). C, plasma (■) and brain (□) concentration of CDA54 in rats, 2.5 h after the indicated oral dose, expressed as mean ± S.E. (n = 8–10).

A consequence of high-affinity binding to inactivated channels compared with resting channels should be a drug-dependent shift in the voltage-dependence of steady-state inactivation to more hyperpolarized potentials. This was indeed the case for CDA54 block of $Na_V1.7$, as shown in Fig. 2C. The maximum current available on depolarization from negative holding potentials was reduced by 12% in the presence of 3 μM CDA54, yielding a K_r value of 22 μM for the experiment shown. To accurately measure drug-induced shifts in inactivation requires that the compound equilibrates at each conditioning potential. As seen in Fig. 2A, in the continued presence of CDA54, binding equilibrates with a time constant of 110 s/μM after a step from −100 to −70 mV. Availability curves in control and in 3 μM CDA54 were therefore constructed using 1-min conditioning pulses. Under these conditions, 3 μM CDA54 shifted the midpoint of the steady-state availability curve (V_h) by −10.9 mV. This shift in the voltage-dependence of inactivation was concentration-dependent (Fig. 2D). Application of 1 and 10 μM CDA54 resulted in shifts of −7.5 and −15.6 mV, respectively. Assuming a simple two-state model in which drug can bind with different affinities to either the resting (K_r) or inactivated state (K_i) of the channel, the concentration-dependence of the shift in V_h is described by the equation $\Delta V_h = k \times \ln\{[1 + ([drug]/K_r)]/([1 + ([drug]/K_i)])\}$, where k is the slope of the Boltzmann equation describing the availability curve (Bean et al., 1983). The line in Fig. 2D represents the fit of the data to this equation for k = −6.3 mV, the average slope of control availability curves, and K_r = 11.4 μM, yielding K_i = 0.46 μM. This value of K_i is slightly greater than that determined from the experiments in Fig. 2B, presumably because of the slow association kinetics, resulting in an underestimate of the shift in V_h at the lower concentrations.

CDA54 did not affect the kinetics of channel activation or inactivation. When the current remaining in the presence of 10 μM CDA54 (11% of control at −70 mV) was scaled (gray trace) to match the amplitude of the current in the absence of compound (black trace), the two traces showed a nearly identical time course (Fig. 2E).

State-Dependence of Block by CDA54. CDA54 displayed use-dependent block of $Na_V1.7$, as shown in Fig. 3A. During 10-Hz stimulation from a holding potential of −100 mV, 3 μM CDA54 caused 83% use-dependent block. Use-dependent or phasic block developed with a time constant of 15 s and was fit well by a single exponential. In another experiment, 3 μM CDA54 yielded 79% block at 10 Hz,

whereas 50 and 91% block were seen with 1 and 10 μM, respectively. Assuming that CDA54 binds equally well to open and inactivated channels during the 6-ms depolarizations and that compound binding and unbinding is slow compared with channel conformational changes, the block observed during 10-Hz stimulation would suggest an affinity for the open and inactivated states of approximately 50 nM, 5-fold more potent than what was observed in the protocols shown in Fig. 2 that favor the inactivated state over the open state. In addition, block developed significantly faster during 10-Hz stimulation, although on average, channels are only open or inactivated 6% of the time compared with 41% of channels residing in the inactivated state during compound application at −70 mV. These data suggest that CDA54 binds with higher affinity and/or faster kinetics to channels in the open state. To test whether CDA54 can efficiently bind to inactivated channels in the absence of channel opening, we took advantage of the slow recovery from inactivated state block. Channels were held at 0 mV, a potential at which all channels were inactivated, for 2 min during which 3 μM CDA54 was bath applied. Figure 3B shows the kinetics of recovery from inactivation after 2 min at 0 mV in control (■) and in 3 μM CDA54 (○). The recovery from inactivation after holding at –60 mV and stimulating at 0.5 Hz is represented by □. When CDA54 was applied to channels in the inactivated state, it produced the characteristic slow recovery, suggesting that block of $Na_V1.7$ by CDA54 does not require channel opening. Taken together, these data suggest that CDA54 binds to channels in the inactivated state with an affinity of 0.25 μM and a slow time course and binds faster and with higher affinity to open channels.

Block of Native and Recombinant $Na_V1.8$ Channels. Block of recombinant $Na_V1.8$ channels stably expressed in HEK-293 cells by CDA54 was both concentration- and voltage-dependent (Fig. 4A). The current evoked by 6-ms depolarizations to 20 mV from −90 mV was blocked 0, 24, and 65% by 1, 3, and 10 μM CDA54, respectively (left), whereas the current evoked by the same test pulse from a holding potential of −60 mV was blocked by 70, 93, and 100% (right). These results are similar to those obtained with $Na_V1.7$, yielding average values of 4.5 ± 0.9 and 0.18 ± 0.02 μM for K_r and K_i, respectively (n = 4).

Figure 4B shows the voltage-dependence of steady-state inactivation in control (squares) and in 10 μM CDA54 (tri-

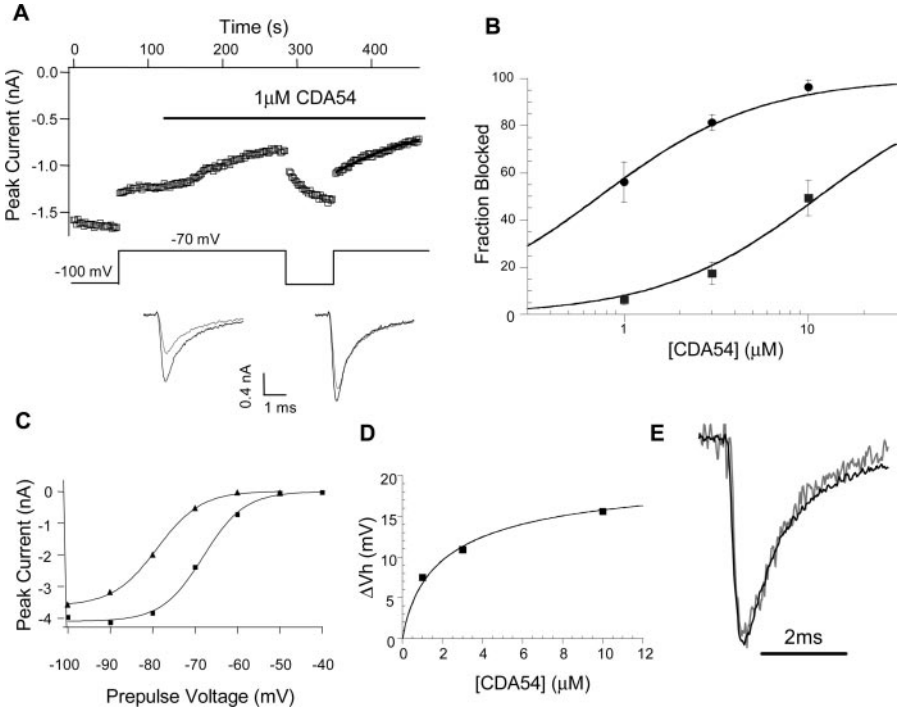

Fig. 2. Block of $hNa_V1.7$ by CDA54. Block of $hNa_V1.7$ channels stably expressed in HEK cells was examined by whole-cell voltage clamp. A, peak current elicited by steps to 0 from −100 or −70 mV (as indicated below the trace) in control and in the presence of 1 μM CDA54. Representative current traces in control and in the presence of 1 μM CDA54 are shown below for −70 mV on the left and −100 mV on the right. B, peak current elicited by steps to 0 mV from either −100 mV (■) or −70 mV (●) was measured in the presence of increasing concentrations of CDA54 and was normalized to the current in the absence of CDA54 (n = 3–8). Fitting the Hill equation (n_H = 1) to the data yielded IC_{50} values of 11.4 and 0.73 μM for holding potentials of −100 and −70 mV, respectively. C, peak current elicited by pulses to 0 mV as a function of prepulse potential in control (■) and in 3 μM CDA54 (▲). Data were best fit by the Boltzmann equation with the following: control, I_{max} = −4.09 nA, V_h = −68.1 mV, k = 4.9 mV; and 3 μM CDA54, I_{max} = −3.61 nA, V_h = −79.0 mV, k = 5.2 mV. D, CDA54-induced shift in the midpoint of availability curves as a function of CDA54 concentration. $\Delta V_h = -6.3\ \text{mV} \times \ln\{[1 + ([\text{CDA54}]/11.4\ \mu\text{M})] / ([1 + ([\text{CDA54}]/K_i)])\}$ best described the data when K_i = 0.46 μM. E, current traces elicited by a step to 0 mV from −70 mV in control (black trace) and in the presence of 10 μM CDA54 (gray trace). Current in CDA54 is scaled to match the amplitude of the control current.

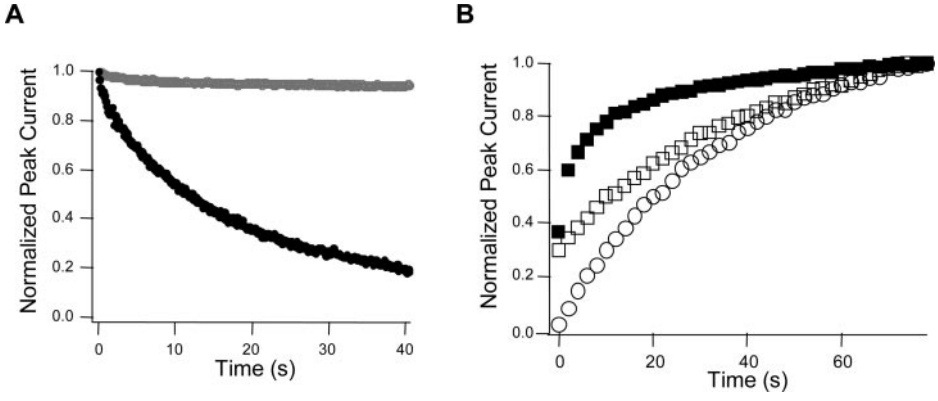

Fig. 3. State-dependence of $hNa_V1.7$ block. A, use-dependent block of $hNa_V1.7$ during 10-Hz stimulation with 6-ms pulses to 0 mV from −100 mV in control (gray trace) and in 3 μM CDA54 (black trace). B, recovery from inactivation upon return to −100 mV after a 2-min period at 0 mV in control (■) or in the presence of 3 μM CDA54 applied at 0 mV (○) or after wash-on of 3 μM CDA54 at −60 mV (□). All symbols represent the peak current during pulses to 0 mV normalized to the current at 80 s. Time constants are 36 s for CDA54 applied at 0 mV and 44 s for CDA54 applied at −60 mV.

angles). In the experiment shown, the maximum current available on depolarization from negative holding potentials was reduced by 40%, and the midpoint of the steady-state availability curve (V_h) was shifted by −27.9 mV, yielding K_r and K_i values of 15 and 0.40 μM, respectively. In this experiment, availability was determined with 1-s conditioning pulses; thus, K_i may be an underestimate.

Small-diameter DRG neurons express two tetrodotoxin-resistant sodium channel subtypes, $Na_V1.8$ and $Na_V1.9$, that can easily be distinguished by the voltage-dependence and kinetics of activation and inactivation. To examine the block of native $Na_V1.8$ channels, dorsal root ganglia from BKTO mice were dissociated, and whole-cell recordings were conducted within 24 to 36 h on small-diameter neurons (10–25 μm) using solutions designed to isolate tetrodotoxin-resistant sodium currents. Under the experimental conditions used, the contribution of $Na_V1.9$ to the peak current was minimal, and Fig. 4C shows representative current traces activated by 40-ms pulses to −10 mV from holding potentials of −60 and −45 mV in the absence and presence of 1 μM CDA54.

Availability curves generated after bath equilibration with 1 μM CDA54 show a reduction in the maximum current activated by pulses to −10 mV from hyperpolarized holding potentials (Fig. 4D), yielding a K_r value of 6.3 ± 1.3 μM (n = 3). Inhibition was more pronounced when currents were activated from more depolarized holding potentials, resulting in an average shift in the steady-state availability curve of −12.4 ± 1.8 mV and an average K_i of 0.09 ± 0.04 μM (n = 3). Because availability was determined with 1-s conditioning pulses, this K_i value may be an underestimate of the true affinity for the inactivated state.

Selectivity of CDA54 for Na_V1 Channels. The selectivity of CDA54 for block of $Na_V1.7$ and $Na_V1.8$ sodium channels was examined by testing effects on $Na_V1.2$ and $Na_V1.5$ channels, using the same protocol described for $Na_V1.7$ channels. CDA54 potently blocked all Na_V1 subtypes tested, and results are summarized in Table 1.

Because voltage-gated sodium and calcium channels are structurally related, and N-type calcium channels are involved in nociception, we tested CDA54 on recombinant $Ca_V2.2$ (a_{1B}, a_2-d, β_{3a}) channels. In whole-cell voltage-clamp experiments, using a standard protocol (15-ms test pulses to 20 mV applied at 0.2 Hz from a holding potential of −90 mV), 3, 10, and 30 μM CDA54 blocked $Ca_V2.2$ by 35% (n = 1), 61 ± 5% (n = 4), and 88 ± 4% (n = 3), respectively, yielding an IC_{50} value of 5.7 μM. The protocol used in these experiments favors the resting state of the channel. Because CDA54 blocked the inactivated state of sodium channels more potently than the resting state, we examined the block of $Ca_V2.2$ at a holding potential of −50 mV, at which 25 to 30% of channels reside in the inactivated state. Under these conditions, the IC_{50} value for block by CDA54 was 3.7 ± 0.2 μM (n = 4), suggesting only a slight preference for block of inactivated $Ca_V2.2$ channels and significant selectivity for $Na_V1.7$ and $Na_V1.8$ over $Ca_V2.2$ channels.

Effects of CDA54 on Nerve Injury-Induced Spontaneous Activity and A- and C-Fiber Conduction. Injury of the sciatic nerve elicits spontaneous action potentials in C-fibers, which can be recorded in vitro (Tal and Devor, 1992).

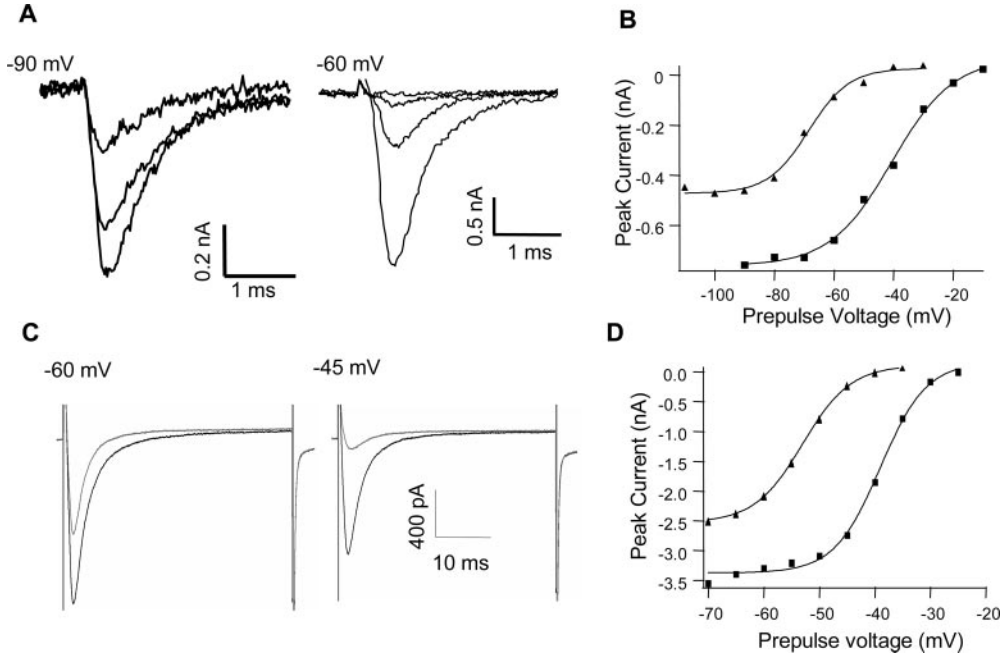

Fig. 4. Block of recombinant and native $Na_V1.8$ channels. A, block of $hNa_V1.8$ channels stably expressed in HEK cells. Current traces elicited by 6-ms pulses to 20 mV: left, in control and in 3 and 10 μM CDA54 from a holding potential of −90 mV; right, in control and in 1, 3, and 10 μM CDA54 from a holding potential of −60 mV. B, peak $hNa_V1.8$ current elicited by pulses to 20 mV as a function of prepulse potential in control (■) and in 10 μM CDA54 (▲). The Boltzmann equation was fit to the data and yielded the following values: in control, I_{max} = −0.83 nA, V_h = −40.7 mV, k = 10.3 mV; and in 10 μM CDA54, I_{max} = −0.50 nA, V_h = −68.5 mV, k = 6.8 mV. C, block of tetrodotoxin-resistant sodium current in dissociated small-diameter mouse DRGs. Current traces elicited by 40-ms pulses to −10 mV from holding potentials of −60 to −45 mV in control and in 1 μM CDA54. D, peak current elicited by pulses to −10 mV as a function of prepulse potential in control (■) and in 1 μM CDA54 (▲). The Boltzmann equation was fit to the data, yielding the following values: in control, I_{max} = −3.38 nA, V_h = −39.0 mV, k = 4.2 mV; and in 1 μM CDA54, I_{max} = −2.53 nA, V_h = −53.0 mV, k = 4.3 mV.

To examine the effect of CDA54 on this injury-induced spontaneous action potential firing, the sciatic nerves from four rats were isolated 2 to 4 weeks after nerve injury and placed into a three-chambered perfusion bath. Using standard teased-fiber recording techniques, C-fibers with regular spontaneous activity were identified. Levels of spontaneous activity remained stable during the 15-min baseline period and during vehicle application. As illustrated in Fig. 5, application of 3 μM CDA54 reduced injury-induced spontaneous activity in 14 C-fibers from 6 animals to 13 $\pm$ 11% of baseline activity, compared with 114 $\pm$ 35% during vehicle application ($p < 0.01$). In the same fibers, in the presence of 3 μM CDA54, electrical stimulation evoked action potentials of the same amplitude as the spontaneous activity during vehicle application. In contrast to the effects on spontaneous activity, 3- to 10-fold higher concentrations of CDA54 were required to inhibit A- and C-fiber electrically evoked responses (Fig. 5). The magnitude of the C-fiber response was reduced by 10 μM ($p < 0.05$) and the A-fiber response by 30 μM CDA54 ($p < 0.01$).

Efficacy in Rat Models of Neuropathic Pain. The original disclosure of CDA54 demonstrated analgesic efficacy of this compound in the formalin test, a rat model of inflammatory pain (Shao et al., 2005). Here, CDA54 was examined for antiallodynic efficacy in the spinal nerve ligation (SNL) and CCI models of neuropathic pain. Two weeks after the SNL injury, mechanical allodynia of the injured hindpaw was assessed by determining withdrawal thresholds in response to stimulation with von Frey filaments. CDA54 produced a dose-dependent reversal of mechanical allodynia (Fig. 6A). A single 3 mg/kg p.o. dose completely reversed mechanical allodynia in one rat but was without effect in most animals, resulting in an average reversal of 19% ($n = 8$), which was not significant. CDA54 at 10 and 30 mg/kg ($n = 8$ each) reversed mechanical allodynia by 44 and 50%, respectively, and increased the percentage of animals responding to the treatment. Treatment with mexiletine, at 100 mg/kg p.o. ($n = 8$), reversed mechanical allodynia by 44% but failed to reach significance because of the number of nonresponders. In the CCI model of neuropathic pain, mechanical hyperalgesia was assessed 2 weeks after injury by determining withdrawal thresholds in response to pressure on the injured (ipsilateral) hindpaw, relative to the uninjured (contralateral) hindpaw. As shown in Fig. 6B, CDA54, administered orally at 10 mg/kg, attenuated the injury-induced mechanical hyperalgesia by 67% ($n = 10$) at 2 h postdose ($p < 0.05$). At 2.5 h postdose, plasma concentrations of CDA54 were 1.69 $\pm$ 0.34 μM. For comparison, mexiletine, at 100 mg/kg p.o. ($n = 11$), did not significantly reverse mechanical hyperalgesia.

Effects on Motor-Coordination and Acute Nociception. Consistent with its low brain penetration, CDA54, at 10 and 30 mg/kg p.o., did not affect motor coordination in rats as judged by the rotorod test (Fig. 6C). In contrast, mexiletine, at the subefficacious dose of 100 mg/kg p.o., significantly reduced walking time on the rotorod. CDA54 was tested in rats for adverse effects on acute nociception. A 10 mg/kg p.o. dose of CDA54 did not alter acute thermal nociception, measured in the hot plate test. Before and 1 h after dosing with CDA54, rats exhibited latencies on a 52.5°C hot plate of 10.5 $\pm$ 0.7 and 9.3 $\pm$ 1.0 s ($n = 6$), respectively.

Effects on Cardiac Electrophysiological Parameters. In the presence of CDA54, channels recover slowly from the inactivated state block after return to hyperpolarized membrane potentials (Fig. 2A). We therefore examined CDA54 for electrocardiographic and cardiac electrophysiological effects in anesthetized dogs, compared with matched vehicle controls (Table 2). Sequential intravenous infusions of 0.25 and 2.5 mg/kg CDA54 yielded plasma levels of 1.31 $\pm$ 0.04 and 6.7 $\pm$ 1.5 μM, respectively, at the time of postdose electrocardiogram and cardiac electrophysiological assessment. At these plasma levels, CDA54 produced no significant effects on heart rate or electrocardiogram intervals, including QRS interval, an index of ventricular conduction, AH interval, a measure of AV nodal conduction, and HV interval, a measure of His-Purkinje ventricular conduction. Likewise, at these plasma levels, CDA54 produced no significant change in atrial or ventricular refractory periods, compared with matched vehicle controls. In contrast, intravenous infusion of

TABLE 1
CDA54 block of $Na_V1.2$, $Na_V1.5$, $Na_V1.8$, and $Na_V1.7$ channels
Data are presented as mean $\pm$ S.E.M.

	K_r	n	K_i	n
	μM		μM	
$Na_V1.2$	20.0 $\pm$ 6.4	5	0.43 $\pm$ 0.03	7
$Na_V1.5$	8.2 $\pm$ 3.2	4	0.15 $\pm$ 0.01	5
$Na_V1.7$	11.4 $\pm$ 1.2	17	0.25 $\pm$ 0.02	17
$Na_V1.8$	4.47 $\pm$ 0.88	4	0.18 $\pm$ 0.02	3

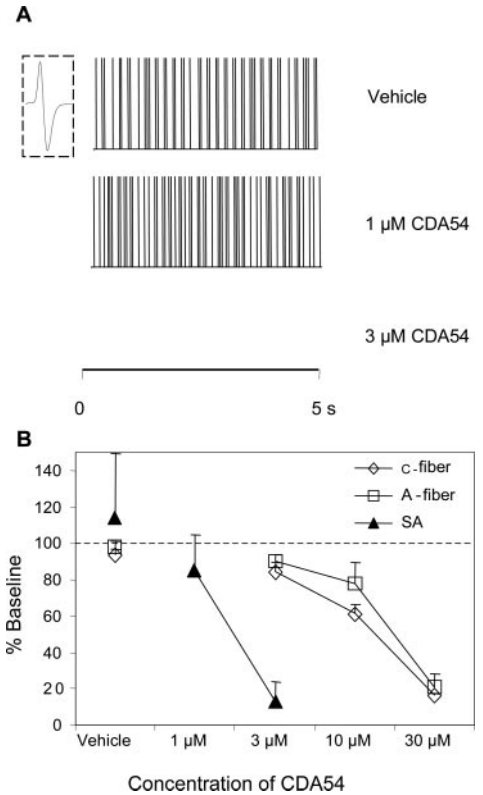

Fig. 5. Block of spontaneous and evoked electrical activity in an isolated nerve after chronic constriction injury. A, injury-induced spontaneous C-fiber action potential firing. Inset, action potential shape is shown. The spontaneous activity was unaffected by vehicle but was completely abolished by 3 μM CDA54. B, CDA54 significantly reduced spontaneous C-fiber action potential firing (SA) at concentrations of 3 μM ($p < 0.01$; $n = 14$ C-fibers), whereas A- and C-fiber electrically evoked conduction was only affected by concentrations of 10 to 30 μM ($p < 0.05$; $n = 6$ nerves). All data are normalized to the baseline response.

3 mg/kg mexiletine, resulting in plasma levels of 24.6 ± 10.2 μM (n = 3), significantly slowed heart rate by 18% and increased PR and QRS intervals by 6% each.

Discussion

Here we describe in vitro and in vivo properties of CDA54, a potent sodium channel blocker that selectively inhibits injury-induced nerve signaling and behavioral signs of neuropathic pain. CDA54 inhibited all Na_V1 channels tested ($Na_V1.2$, $Na_V1.5$, $Na_V1.7$, and $Na_V1.8$) in a state- and frequency-dependent manner, and was selective for Na_V1 channels over N-type calcium channels. The compound displayed a low brain-to-plasma ratio of 0.03, suggesting that CDA54 acts peripherally. In vivo, CDA54 displayed efficacy in the rat spinal nerve ligation and chronic constriction injury models of neuropathic pain at doses and plasma concentrations that did not affect motor coordination, acute nociception, or cardiac conduction. In contrast, at doses that disrupt motor coordination, mexiletine failed to significantly reduce neuropathic pain behavior.

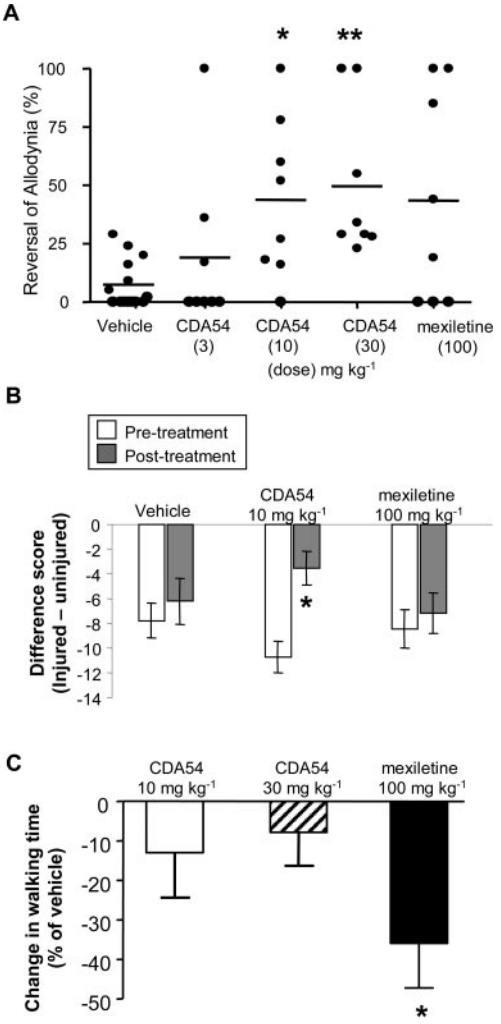

Fig. 6. Effect of CDA54 in rat models of neuropathic pain and motor coordination. A, 1 week after spinal nerve ligation, mechanical allodynia was assessed with calibrated von Frey filaments before and after oral administration of vehicle, CDA54, or mexiletine. Reversal of injury-induced mechanical allodynia is shown for each animal tested. *, $p < 0.05$, and **, $p < 0.01$, Dunnett's multiple comparison after ANOVA. B, mechanical hyperalgesia was examined in response to paw pressure 1 week after chronic constriction. The difference in mechanical thresholds between the injured and uninjured paw are plotted after oral administration of vehicle, CDA54, or mexiletine. *, $p < 0.05$, unpaired t test. C, motor coordination was evaluated on the rotorod after oral administration of CDA54 or mexiletine. Compared with vehicle, walking times were reduced by 13.0 ± 11.4 and 7.8 ± 8.6% for 10 and 30 mg/kg CDA54, respectively (n = 5 each) and by 35.9 ± 11.4% for 100 mg/kg mexiletine (n = 7). *, $p < 0.05$, unpaired t test.

CDA54 seems to bind predominantly to channels in open and inactivated states, similar to local anesthetics, such as lidocaine and tetracaine. Binding to the inactivated state of $Na_V1.7$ is approximately 30-fold more potent than binding to the resting state, and data comparing different pulse protocols suggest that binding to the open state may be even more potent. This type of state-dependence allows channels to open normally during brief depolarizations from the resting membrane potential, suggesting minimal impact on normal nerve conduction. Damage to peripheral nerves can induce a physiological state in which spontaneous action potential firing occurs in normally silent sensory neurons. This abnormal peripheral nerve activity is believed to contribute to the perception of neuropathic pain. Sodium channels clearly play a key role in the initiation and propagation of this spontaneous activity. In vitro, CDA54 inhibits this spontaneous firing at lower concentrations that those required to block normal A- and C-fiber conduction, similar to what has been observed for systemic administration of lidocaine in in vivo recordings (Devor et al., 1992). What makes the injury-induced spontaneous firing more sensitive to inhibition by sodium channel blockers is unclear. It is possible that spontaneous firing in DRGs is dependent on a persistent, subthreshold sodium current. In large-diameter neurons, late sodium current has been shown to be more sensitive to block by local anesthetics than the peak current (Baker, 2000). For this late current to be involved in ectopic impulse generation, sodium channels would have to remain open at the resting membrane potential. Because open channels are highly sensitive to block by CDA54, ectopic impulses initiated by subthreshold sodium current should be readily blocked by CDA54. Second, the membrane potential in injured neurons may be more depolarized than in uninjured neurons, favoring inactivation and thus favoring block by CDA54. A more depolarized membrane potential of injured dissociated neurons has been found by some groups (Kim et al., 1998) but not by others (Study and Kral, 1996; Zhang et al., 1997; Abdulla and Smith, 2001). However, a caveat of these studies is that the electrical properties of the cell body may not reflect those at

TABLE 2

Effect of CDA54 (sequential 0.25 and 2.5 mg/kg i.v. infusion) on electrocardiographic and cardiac electrophysiological parameters in anesthetized dogs

For all parameters, data are presented as mean ± S.E.M. (n = 3).

	CDA54		
	Baseline	0.25 mg/kg i.v.	2.5 mg/kg i.v.
Sinus heart rate (bpm)	107 ± 2	105 ± 0	102 ± 2
PR interval (ms)	95 ± 7	98 ± 7	101 ± 7
QRS interval (ms)	53 ± 2	53 ± 2	54 ± 3
QTc interval (ms/$\sqrt{s}$)	393 ± 29	397 ± 28	395 ± 30
AH interval (ms)	85 ± 5	86 ± 6	91 ± 6
HV interval (ms)	22 ± 2	22 ± 2	22 ± 2
Atrial RRP (ms)	139 ± 9	141 ± 8	147 ± 9
Ventricular RRP (ms)	173 ± 9	173 ± 7	173 ± 6

bpm, beats per minute.

the site of injury. Finally, slight disturbances in the balance between depolarizing sodium currents and hyperpolarizing potassium currents may lead to spontaneous firing and require only a small reduction in available sodium current to restore the preinjury balance. Indeed, potassium channel blockers such as 4-amino pyridine can induce spontaneous firing in vitro (Kocsis et al., 1983). In this scenario, one might expect non–state-dependent blockers to be as effective as state-dependent ones. Spontaneous activity (in vitro) of Aβ- and Aδ-fibers after spinal nerve ligation was significantly inhibited by 6.3 nM tetrodotoxin, whereas 500 nM tetrodotoxin was required for conduction block (Liu et al., 2001). In the same study, effective doses of lidocaine ranged from 9.3 to 18.5 μM, with 2 to 7 mM required for conduction block. A similar study, using in vivo recording and systemic application of tetrodotoxin after sciatic nerve transsection, found that the ectopic activity originating from the neuroma was approximately 50-fold more sensitive to tetrodotoxin than activity of dorsal horn neurons (Omana-Zapata et al., 1997). However, interpretation of these studies is complicated by the fact that different Na_V1 subtypes have vastly different sensitivities to block by tetrodotoxin.

Currently used agents are highly brain-penetrant. Whereas block of central nervous system sodium channels by these drugs certainly contributes to their dose-limiting side effects, include ataxia, somnolence, and sedation, it is not clear whether it also contributes to their analgesic efficacy. CDA54 is only weakly brain penetrant, with a brain-to-plasma ratio of 0.03, suggesting that, at least in a rat model of neuropathic pain, block of sodium channel of the peripheral nervous system alone is sufficient for analgesic efficacy.

Although none of the clinically used sodium channel blockers are subtype-selective, in randomized trials of systemically administered sodium channel blockers for prolonged pain, no cardiac side effects were noted. The sparing of cardiac conduction is at least in part caused by a high safety factor, defined as the ratio of the available sodium current to that required to sustain action potential propagation. Despite this safety factor, class Ic antiarrhythmics such as flecainide or propafenone have the potential to induce arrhythmias, especially in patients with prior myocardial infarction (Pratt and Moye, 1990). CDA54 possesses slow kinetics of recovery from inactivated state block, similar to class Ic agents. Based on these findings, CDA54 would be expected to affect cardiac conduction and cause bradycardia. However, in an instrumented cardiovascular dog model, CDA54 was without effect at plasma concentrations of 6.7 μM; concentrations that are approximately 25-fold greater than the K_i for block of $Na_V1.7$ and in the range of therapeutic concentrations in the SNL and CCI models of neuropathic pain. In contrast, mexiletine caused mild bradycardia and increases in PR and QRS intervals at plasma concentrations of 25 μM; approximately 2.5-fold greater than the K_i value for block of $Na_V1.7$ and 2-fold greater than the subefficacious concentrations reached approximately 100 min after a single 100 mg/kg oral dose (11.8 ± 2.6 μM).

In summary, CDA54 seems to block peripheral nerve sodium channels by a mechanism similar to that of clinically used anticonvulsants and antiarrhythmics but approximately 2 orders of magnitude more potent. In vitro, CDA54 blocks all Na_V1 subtypes with similar potency; however, in isolated nerve studies, CDA54 selectively inhibits injury-induced action potential firing. CDA54 also displays functional selectivity in vivo: the same dose of CDA54 that was effective in rat models of neuropathic pain did not affect acute nociception. In addition, no effects on cardiac conduction were observed at plasma concentrations approximately 45-fold greater than the K_i value for block of $Na_V1.5$.

Acknowledgments

We thank Franz Hofmann for the $hNa_V1.7$ cDNA and Hali Hartmann for the cDNA and HEK cells expressing $hNa_V1.5$. We are grateful to Martin Kohler and Chou Liu for use of the cell lines expressing $hNa_V1.2$ and $hNa_V1.8$. Furthermore, we thank Alana Upthagrove for analysis of plasma concentrations, Elizabeth Ash for help with the teased-fiber recordings, and Keith Wafford for advice and helpful discussions.

References

Abdulla FA and Smith PA (2001) Axotomy- and autotomy-induced changes in the excitability of rat dorsal root ganglion neurons. *J Neurophysiol* **85:**630–643.

Akopian AN, Souslova V, England S, Okuse K, Ogata N, Ure J, Smith A, Kerr BJ, McMahon SB, Boyce S, et al. (1999) The tetrodotoxin-resistant sodium channel SNS has a specialized function in pain pathways. *Nat Neurosci* **2:**541–548.

Baker MD (2000) Selective block of late Na^+ current by local anaesthetics in rat large sensory neurones. *Br J Pharmacol* **129:**1617–1626.

Bean BP, Cohen CJ, and Tsien RW (1983) Lidocaine block of cardiac sodium channels. *J Gen Physiol* **81:**613–642.

Bennett GJ and Xie YK (1988) A peripheral mononeuropathy in rat that produces disorders of pain sensation like those seen in man. *Pain* **33:**87–107.

Campbell JN and Meyer RA (1983) Sensitization of unmyelinated nociceptive afferents in monkey varies with skin type. *J Neurophysiol* **49:**98–110.

Chaplan SR, Bach FW, Pogrel JW, Chung JM, and Yaksh TL (1994) Quantitative assessment of tactile allodynia in the rat paw. *J Neurosci Methods* **53:**55–63.

Chaplan SR, Bach FW, Shafer SL, and Yaksh TL (1995) Prolonged alleviation of tactile allodynia by intravenous lidocaine in neuropathic rats. *Anesthesiology* **83:**775–785.

Clare JJ, Tate SN, Nobbs M, and Romanos MA (2000) Voltage-gated sodium channels as therapeutic targets. *Drug Discov Today* **5:**506–520.

Devers A and Galer BS (2000) Topical lidocaine patch relieves a variety of neuropathic pain conditions: an open-label study. *Clin J Pain* **16:**205–208.

Devor M, Wall PD, and Catalan N (1992) Systemic lidocaine silences ectopic neuroma and DRG discharge without blocking nerve conduction. *Pain* **48:**261–268.

Hamill OP, Marty A, Neher E, Sakmann B, and Sigworth FJ (1981) Improved patch-clamp techniques for high-resolution current recording from cells and cell-free membrane patches. *Pflueg Arch Eur J Physiol* **391:**85–100.

Hille B (1977) Local anesthetics: hydrophilic and hydrophobic pathways for the drug-receptor reaction. *J Gen Physiol* **69:**497–515.

Hondeghem LM and Katzung BG (1977) Time- and voltage-dependent interactions of antiarrhythmic drugs with cardiac sodium channels. *Biochim Biophys Acta* **472:**373–398.

Igwemezie LN, Beatch GN, McErlane KM, and Walker MJ (1992) Mexiletine's antifibrillatory actions are limited by the occurrence of convulsions in conscious animals. *Eur J Pharmacol* **210:**271–277.

Kajander KC and Bennett GJ (1992) Onset of a painful peripheral neuropathy in rat: a partial and differential deafferentation and spontaneous discharge in A beta and A delta primary afferent neurons. *J Neurophysiol* **68:**734–744.

Khasar SG, Gold MS, and Levine JD (1998) A tetrodotoxin-resistant sodium current mediates inflammatory pain in the rat. *Neurosci Lett* **256:**17–20.

Kim SH and Chung JM (1992) An experimental model for peripheral neuropathy produced by segmental spinal nerve ligation in the rat. *Pain* **50:**355–363.

Kim YI, Na HS, Kim SH, Han HC, Yoon YW, Sung B, Nam HJ, Shin SL, and Hong SK (1998) Cell type-specific changes of the membrane properties of peripherally-axotomized dorsal root ganglion neurons in a rat model of neuropathic pain. *Neuroscience* **86:**301–309.

Kocsis JD, Ruiz JA, and Waxman SG (1983) Maturation of mammalian myelinated fibers: changes in action-potential characteristics following 4-aminopyridine application. *J Neurophysiol* **50:**449–463.

Kuo CC and Bean BP (1994) Slow binding of phenytoin to inactivated sodium channels in rat hippocampal neurons. *Mol Pharmacol* **46:**716–725.

Lai J, Gold MS, Kim CS, Bian D, Ossipov MH, Hunter JC, and Porreca F (2002) Inhibition of neuropathic pain by decreased expression of the tetrodotoxin-resistant sodium channel, NaV1.8. *Pain* **95:**143–152.

Laird JM, Souslova V, Wood JN, and Cervero F (2002) Deficits in visceral pain and referred hyperalgesia in Nav1.8 (SNS/PN3)-null mice. *J Neurosci* **22:**8352–8356.

Liu CN, Wall PD, Ben-Dor E, Michaelis M, Amir R, and Devor M (2000) Tactile allodynia in the absence of C-fiber activation: altered firing properties of DRG neurons following spinal nerve injury. *Pain* **85:**503–521.

Liu X, Zhou JL, Chung K, and Chung JM (2001) Ion channels associated with the ectopic discharges generated after segmental spinal nerve injury in the rat. *Brain Res* **900:**119–127.

Nakazono T, Murakami T, Higashi Y, and Yata N (1991) Study on brain uptake of local anesthetics in rats. *J Pharmacobiodyn* **14:**605–613.

Nassar MA, Stirling LC, Forlani G, Baker MD, Matthews EA, Dickenson AH, and

Wood JN (2004) Nociceptor-specific gene deletion reveals a major role for Nav1.7 (PN1) in acute and inflammatory pain. *Proc Natl Acad Sci USA* **101:**12706–12711.
Omana-Zapata I, Khabbaz MA, Hunter JC, Clarke DE, and Bley KR (1997) Tetrodotoxin inhibits neuropathic ectopic activity in neuromas, dorsal root ganglia and dorsal horn neurons. *Pain* **72:**41–49.
Pratt CM and Moye LA (1990) The Cardiac Arrhythmia Suppression Trial: background, interim results and implications. *Am J Cardiol* **65:**20B–29B.
Priest BT, Garcia ML, Middleton RE, Brochu RM, Clark S, Dai G, Dick IE, Felix JP, Liu CJ, Reiseter BS, et al. (2004) A disubstituted succinamide is a potent sodium channel blocker with efficacy in a rat pain model. *Biochemistry* **43:**9866–9876.
Priest BT, Murphy BA, Lindia JA, Diaz C, Abbadie C, Ritter AM, Liberator P, Iyer LM, Kash SF, Kohler MG, et al. (2005) Contribution of the tetrodotoxin-resistant voltage-gated sodium channel Na(v)1.9 to sensory transmission and nociceptive behavior. *Proc Natl Acad Sci USA* **102:**9382–9387.
Renganathan M, Cummins TR, and Waxman SG (2001) Contribution of Na(v)1.8 sodium channels to action potential electrogenesis in DRG neurons. *J Neurophysiol* **86:**629–640.
Shao PP, Ok D, Fisher MH, Garcia ML, Kaczorowski GJ, Li CS, Lyons KA, Martin WJ, Meinke PT, Priest BT, et al. (2005) Novel cyclopentane dicarboxamide sodium channel blockers as a potential treatment for chronic pain. *Bioorg Med Chem Lett* **15:**1901–1907.
Study RE and Kral MG (1996) Spontaneous action potential activity in isolated dorsal root ganglion neurons from rats with a painful neuropathy. *Pain* **65:**235–242.
Stump GL, Smith GR, Tebben AJ, Jahansouz H, Salata JJ, Selnick HG, Claremon DA, and Lynch JJ Jr (2003) In vivo canine cardiac electrophysiologic profile of 1,4-benzodiazepine IKs blockers. *J Cardiovasc Pharmacol* **42:**105–112.
Tal M and Devor M (1992) Ectopic discharge in injured nerves: comparison of trigeminal and somatic afferents. *Brain Res* **579:**148–151.
Tanelian DL and Brose WG (1991) Neuropathic pain can be relieved by drugs that are use-dependent sodium channel blockers: lidocaine, carbamazepine and mexiletine. *Anesthesiology* **74:**949–951.
Yang Y, Wang Y, Li S, Xu Z, Li H, Ma L, Fan J, Bu D, Liu B, Fan Z, et al. (2004) Mutations in SCN9A, encoding a sodium channel alpha subunit, in patients with primary erythermalgia. *J Med Genet* **41:**171–174.
Yoshimura N, Seki S, Novakovic SD, Tzoumaka E, Erickson VL, Erickson KA, Chancellor MB, and de-Groat WC (2001) The involvement of the tetrodotoxin-resistant sodium channel Na(v)1.8 (PN3/SNS) in a rat model of visceral pain. *J Neurosci* **21:**8690–8696.
Zhang JM, Donnelly DF, Song XJ, and Lamotte RH (1997) Axotomy increases the excitability of dorsal root ganglion cells with unmyelinated axons. *J Neurophysiol* **78:**2790–2794.

Address correspondence to: Dr. Birgit Priest, Merck and Co, Inc., 126 E. Lincoln Ave, RY80N-C31, P.O. Box 2000, Rahway, NJ 07065-0900. E-mail: birgit_priest@merck.com